

Domain Independent Adaptive Histogram Based Features for Pomegranate Fruit and Leaf Diseases Classification

Double blind

Abstract

Disease identification for fruits and leaves in the field of agriculture is important for estimating production, crop yield and earnings for farmers. In the specific case of pomegranates, this is challenging because of the wide range of possible diseases and their effects on the plant and the crop. This study presents an adaptive histogram-based method for solving this problem. Our method describe is domain independent in the sense that it can be easily and efficiently adapted to other similar smart agriculture tasks. The approach explores color spaces, namely, Red, Green, and Blue along with Gray. The histograms of color spaces and gray space are analyzed based on the notion that as the disease changes, the color also changes. The proximity between the histograms of gray images with individual color spaces is estimated to find the closeness of images. Since the gray image is the average of color spaces (R, G, and B), it can be considered a reference image. For estimating the distance between gray and color spaces, the proposed approach uses a Chi-Square distance measure. Further, the method uses an Artificial Neural Network for classification. The effectiveness of our approach is demonstrated by testing on a dataset of fruit and leaf images affected by different diseases. The results show that the method outperforms existing techniques in terms of average classification rate.

Keywords: Color spaces, Distance measure, Fruit classification, Leaf classification, Plant disease classification.

1. Introduction

When we look at the history and effect of agricultural diseases, there is a tremendous impact on production which places a financial burden on farmers. Out of many such diseases, the Bacterial blight, caused by *Xanthomonas axonopodis* pv. *Punicae* [1-4], poses a significant threat. Since 2012, this disease has reached critical levels, severely affecting India's economy, particularly the export of quality fruits. Due to the disease's impact, pomegranate production in India had dropped by 60% following an outbreak that resulted in a 70-100% loss in the states of Karnataka and Maharashtra during 2021 [1-4].

Pomegranate production in Karnataka has experienced a significant decline, plummeting from a peak of 180,000 metric tonnes annually four years earlier to less than 10,000 metric tonnes in the 2017-18 season. This drastic reduction has resulted in a staggering revenue loss of approximately Rs. 200 crores (calculated at an average price of Rs. 50,000 per tonne). A survey conducted in Karnataka highlighted disease severity ranging from 20% to 90% in the Bijapur and

Bagalkot districts, while more recent reports indicated varying severity levels, with the highest being 74.80% in the Bagalkot district and the lowest at 6.73% in the Bellary district. By the 2018-19 season, the disease had reached a critical stage, inflicting substantial damage on the crop and causing significant losses for farmers. A severe case of Bacterial blight produces a 50-100 % reduction in pomegranate output. Thrips and aphids are a nuisance that may be found in all of the Solapur districts. One can understand from the above statistical analysis that there is an urgent need for developing a simple and effective model for disease identification such that there can be reduction in losses and preservation of quality of life for farmers in Karnataka, Maharashtra, India. This is our main motivation for developing a model for disease classification for pomegranates as described in this paper.

When we look at past and present agriculture, disease classification for pomegranates based on images of fruits and leaves has gained significant attention as a way of increasing production and profits [5-15]. This is because the pomegranate crop has become a commercial crop and it is the main source of income for millions of farmers in Karnataka, India compared to other fruits and vegetables [16, 17]. Recent changes in weather and natural disasters have also impacted crop production across the whole Karnataka region [17].

A key challenge is the rise of different new diseases, which prevent the ripening of quality pomegranates and lower the yield [16, 17]. Our approach is aimed at automatically identifying different diseases of the pomegranate fruit, namely, Deep Splitting, Light Splitting, Translucent Black and Necrotic Dark Brown, and diseases of the pomegranate leaves, namely, Necrotic Soaked Spots, Chlorosis, Light Green Spots, Necrosis, and White Patches. It is noted from the literature that these diseases are common across states and countries, causing major damage to crops [17]. Sample images of fruit showing different diseases are shown in Fig. 1(a) and diseases of leaves are shown in Fig. 1(b), where it can be seen the effects of the different diseases have characteristic patterns in terms of color, shape, and texture, etc. The same is true for the images of leaves affected by different diseases shown in Fig. 1(b). It is also observed from Fig. 1(a) and Fig. 1(b) that some diseases share characteristics. For instance, the pattern and color of Translucent Black share the same features as Necrotic Dark Brown in the case of fruit. Similarly, one can see common properties in Necrotic Soaked Spots, Light Green Spots and Necrosis leaf images in Fig. 1(b). This shows that the identification of fruits and leaves suffering from different diseases is not easy because of a lack of discriminative cues.

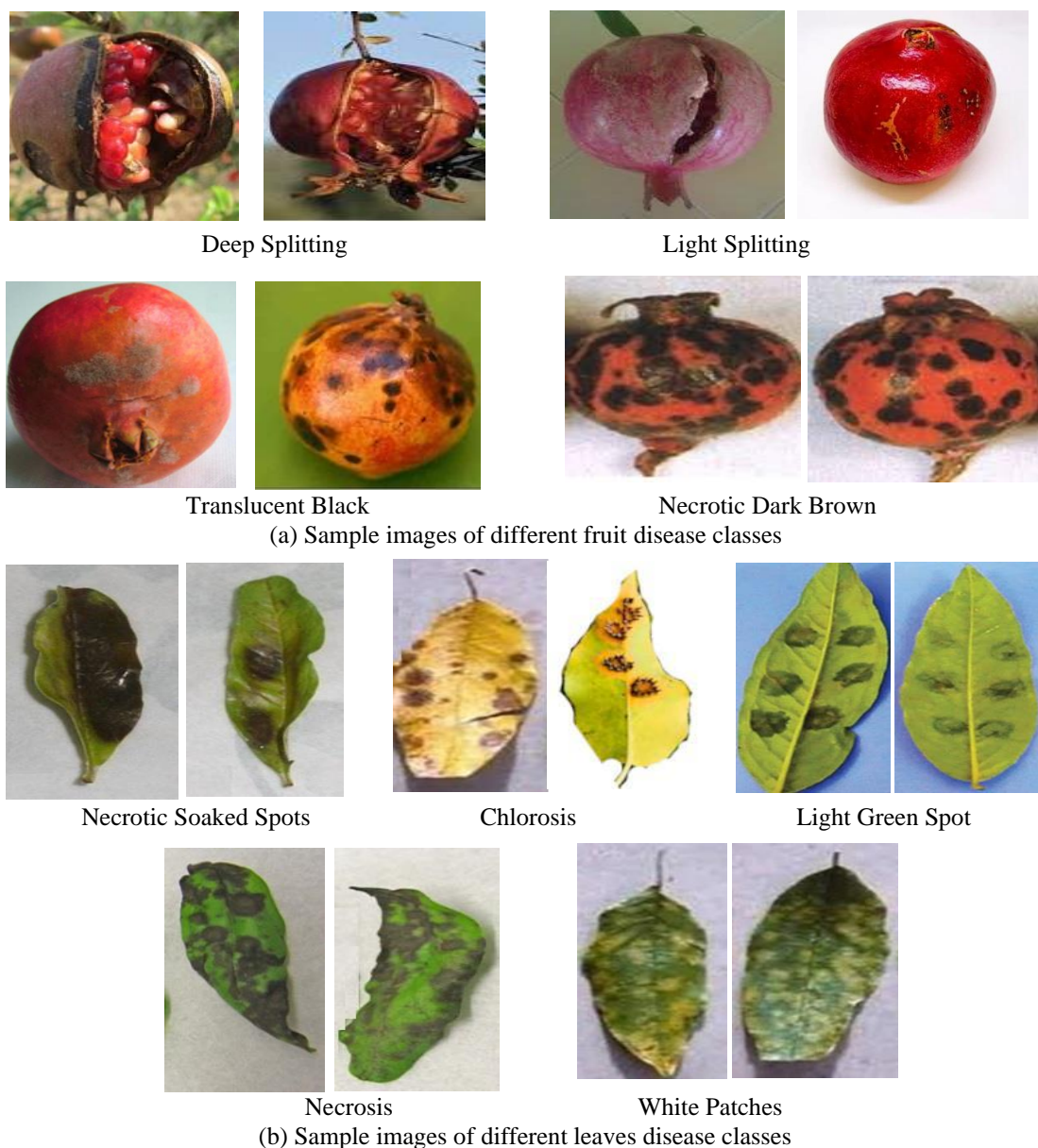


Fig.1. Examples of different pomegranate fruits and leaves disease classes.

Hence, disease identification for pomegranates is challenging. In addition, adding the classification of pomegranate leaf diseases which are different from fruits diseases adds complexity. In the past, methods have been developed for disease identification in pomegranate fruits and leaves [17, 18]. However, these methods are not robust because the models focus on specific domains, but not on fruit and leaf diseases in combination. For this reason, the problem of classification of pomegranate and leaf diseases can be considered an open challenge.

The aim of this work is to identify diseases automatically at early stages so that farmers can prevent damage by spraying pesticides and remove affected fruit and leaves to prevent spreading the disease. In this way, our proposed method can assist farmers in growing pomegranate, helping them to increase production and yield. Our work focuses on introducing a new method based on

adaptive histogram features using color spaces of the input images and an artificial neural network for classification. It can be seen from Fig. 1(a) and Fig. 1(b) that for different diseases of fruits and leaves, the color, shape of the patches, and degradations are important in differentiating the diseases. This observation motivated us to introduce histogram-based features to extract discriminative features for classification. The histograms are drawn using color spaces, namely, Red, Green, Blue, and gray components.

To extract the shape and degradations from the input images, we locate a dominant peak in the histograms that divides the whole histogram into two equal halves. This makes sense because when the shape of the patches and their quality changes, the same changes are reflected in the peaks and two halves of the histogram. We believe that these extracted features have sufficient discriminative power to classify the different diseases irrespective of domains (fruits and leaves). We use a simple Artificial Neural Network for classification. Because collecting a large number of real samples and annotations requires substantial effort and time, our approach explores the combination of handcrafted features and simple classifiers rather than deep learning-based models. Our goal is to develop a simple and effective method that can be implemented in a real time environment. In addition, we believe that although deep learning models generally achieve high accuracies, their generalizability to unexpected inputs (outliers) can be problematic in contrast to feature-based methods [19, 20]. When we focus on the practical implications of our proposed approach, we note that it out-performs other state-of-the-art methods.

The effectiveness of deep learning models is offset by the difficulty and expense of collecting and labeling sufficient training data. Without enough training data, such approaches tend to be “brittle,” especially given the large degree of variation in plant disease states. Our application demands a low-cost approach that is robust in the presence of outliers.

We believe that exploring the application of basic concepts to solving complex problems is in itself a contribution. Extending existing approaches that are efficient to new challenges saves energy, time, and resources. In certain situations, like the one under study, this may be sufficient, and more complicated techniques are not justified. Simpler approaches also facilitate reproducibility, which is an important consideration nowadays. We believe these key points provide novelty and add to the impact of our work.

The key contributions in this paper are as follows. (i) We believe that this is the first work to address the challenges of both fruit and leaf disease classification with a single method. In other words, proposing a domain-independent approach for disease identification is new compared to the state-of-the-art. (ii) For extracting domain-independent features, exploring the histograms

approach is a novel idea. (iii) In particular, combining color histograms and gray histograms using Chi-Square distance is another contribution.

The structure of the paper is as follows. A review of existing methods for fruit and leaf disease classification is presented in Section 2. Section 3 describes the proposed histogram-based approach for feature extraction. Experimental results on the fruit and leaf image dataset are presented along with a comparative study of existing methods appears in Section 4. Section 5 concludes with our findings and discusses future research.

2. Related Work

If we consider fruit and leaf disease identification as an image classification problem, we can point to several methods developed in the past [21-24]. However, the main objective of these methods is aimed at classifying object in the images without focusing on particular regions which provide cues about a disease. Therefore, these methods may not be suitable for pomegranates and our leaf disease classification problem. The general features extracted by the image classification methods may not be effective for disease region representation. As noted previously, we also seek approaches that can operate successfully without a lot of training data, which is expensive to gather and label. These points will be a focus when we present our experimental results later in this paper.

Thus, the state-of-the art for disease identification is divided into two sub-sections. Pomegranate fruit disease classification and leaf disease classification. These methods use both handcrafted features and deep learning models for classification.

2.1. Fruit Disease Identification

Pradeep et al. [25] proposed a method for fruit disease classification based on a convolutional neural network. The approach focuses on training the model without a large number of samples and it considers orange fruit for classification. However, the method is tested and validated on only orange fruits because the scope of the mode is limited to specific fruits. Gom-OS [26] proposed a method for fruit classification by exploring colorized depth information. For the classification of different fruits, namely, apples, orange, Mango, banana, and rambutan, the color and depth of image information have been explored. However, the scope of the method is limited to the classification of different fruits and not disease classification. Sajitha et al. [27] proposed a technique for Banana fruit disease detection using a graph convolutional neural network. The method also focuses on exploring deep learning models for classification. Mathboli et al. [28] developed a model for Apple fruit disease identification based convolutional neural network. The

approach focuses on extracting shape features for classification. Mehata et al. [29] used a convolutional neural network for the automatic diagnosis of dragon fruit through a planned photograph. However, the method may work well for particular diseases. Nagesh et al. [30] developed a deep-learning model for the classification of tomato fruit disease. The performance of the method improves through augmentation techniques which generate a large number of samples.

Mallikarjuna et al. [19, 20] used the combination of gradient and deep learning models for the classification of different diseases of arecanut. The gradient-directional information has been used for enhancing the images that suffer from degradations and lost cues for classification. The deep learning approach has been used for feature extraction and classification. However, these models work well for arecanut images, but not pomegranate fruit and leaf images. This is because the scope of the methods is limited to arecanut-diseased images. Koufatzis et al. [31] developed a model for inspecting the visual quality of the fruit images based on a deep learning-based approach. It also classifies different samples based on quality. If a plant is affected by disease, the quality of the image drops. Therefore, the method basically classifies good images and images affected by different diseases. The method considers pomegranate fruit as cases study for evaluating the performance of the method. Kale et al. [32] also made an attempt to assess the visual quality of the pomegranate fruit images based on a neural network. The main focus of the method is to analyze the performance of different methods to assess the quality of the pomegranate fruit images.

In summary, it is noted from the above review that the models used deep learning approaches for fruit disease classification. However, most of the models focus on a particular fruit disease. This suggests that the existing methods do not have generalization ability. In addition, there are some methods for pomegranate disease identification, but the methods do not report satisfactory results for different diseases of pomegranates.

2.2. Leaf Disease Identification

Nirmal et al. [17] aim at developing a model for pomegranate disease identification that can run on a smartphone. The authors used different deep learning architectures for analyzing the results of classification. This work considers leaf images for the identification disease of pomegranate fruit. Wakhare et al. [16] presented a study of pomegranate disease identification using leaf images. The main objective of the work is to implement IoT and artificial intelligence to identify the disease of pomegranate plants. The study also discusses the effect of diseases on production and yields. Nirmal et al. [18] proposed the combination of feature extraction and machine learning

for pomegranate leaf disease classification. The approach performs an enhancement operation over the image to enhance the fine details in the image and then employs a segmentation technique to segment the region of interest. Nirmal et al. [33] developed a model based on deep learning for pomegranate plant leaf disease identification. The approach explores the combination of convolutional neural networks and LSTM for feature extraction.

There are methods for pomegranate leaf disease identification. It is noted that none of the methods consider both fruit disease and leaf disease for classification. This shows that methods work well for specific cases and hence may not be domain independent and robust to different datasets.

Overall, it is noted from the review that to increase the production of pomegranates, it is necessary to identify fruit and leaf diseases at an earlier stage. But there are no methods that work for both fruit and leaf diseases. Therefore, one can conclude that there is a demand for developing a single model for classifying diseases of pomegranate fruit and leaves. Thus, this work aims at developing a domain-independent method for disease classification.

3. Proposed Methodology

When we look at sample images of fruits and leaves suffering from different diseases shown in Fig. 1(a) and Fig. 1(b), the variations in terms of texture, patterns of diseased patches, distortion and degradations in the images in the same class is high. At the same time, there is a minute difference between the color and shapes of the patches of the images in the different classes. This is true for both fruit and leaf diseases. This is where the problem becomes more complex and challenging compared to past work in the area. Developing a model that can address these points is an open challenge.

This work considers pomegranate fruit and leaves affected by different diseases as input for disease classification. The fruit diseases are Deep Splitting, Light Splitting, Translucent Black, and Necrotic Dark Brown, which have four classes. The leaf diseases are Necrotic Soaked Spots, Chlorosis, Light Green Spot, Necrosis, and White Patches, which has five classes. It is noted from the literature that these diseases are the main diseases that damage the crops heavily in the field. As noted in Fig. 2(a) and Fig. 3(a), the images share common properties and cues.

To solve this problem, inspired by the observation that the color, shape of the patches, and changes prominently in all the diseases, we introduce a histogram-based approach in different color space for extracting such observation for classification. We believe that for different diseases, the distribution of the histogram's changes in different color spaces as shown in Fig. 2(b-e) and Fig. 3(b-e), respectively. The features are extracted by estimating the distance between

the histogram of color spaces, namely, Red, Green, and Blue, and the histogram of gray images. The reason to consider the gray image for estimating distance features is that the gray image is the average of R, G, and B components, which is considered a reference image as shown in Fig. 2(b) and Fig. 3(b). The reason to explore histogram approach is that the behavior of the histograms can withstand the effect of degradations and background variations. For estimating the distance between histograms of R, G, and B and the histogram of the gray image, we use the Chi-Square distance measure. This is because the Chi-Square distance measure is derived for matching the histograms. The extracted features are fed to Artificial Neural Network (ANN) for classification. The steps and flow of the proposed method can be seen in Fig. 4.

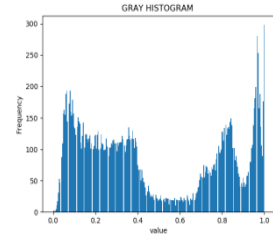
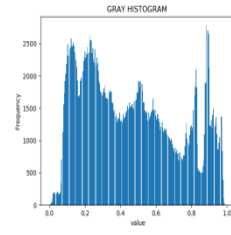
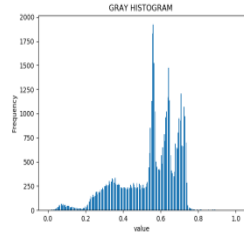
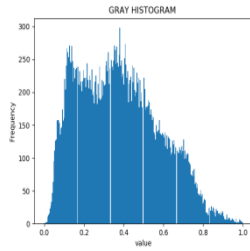


(a) Deep splitting

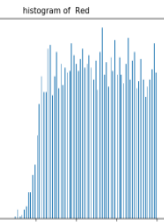
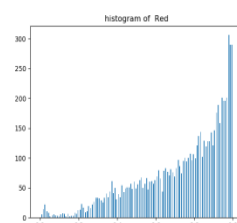
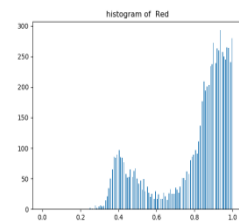
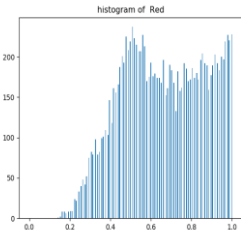
Light splitting

Translucent black

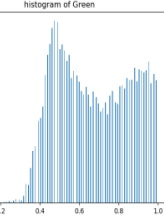
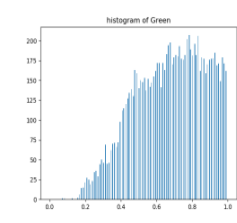
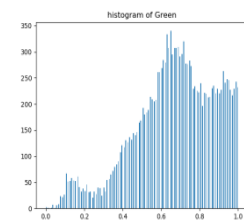
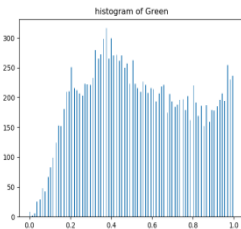
Necrotic dark brown



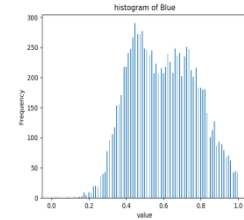
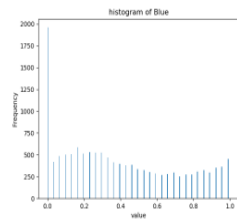
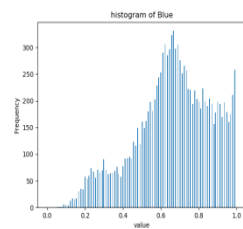
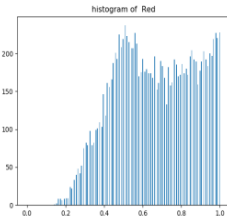
(b) Histograms of gray color space for the images in (a).



(c) Histograms of R color space for all the images in (a)



(d) Histograms of G color space for all the images in (a)

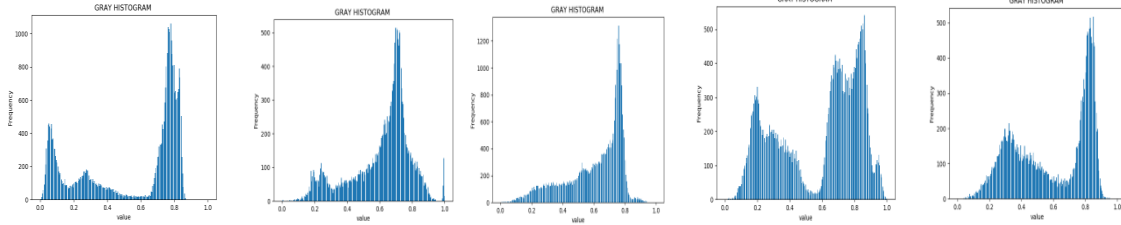


(e) Histograms of B color space for all the images in (a)

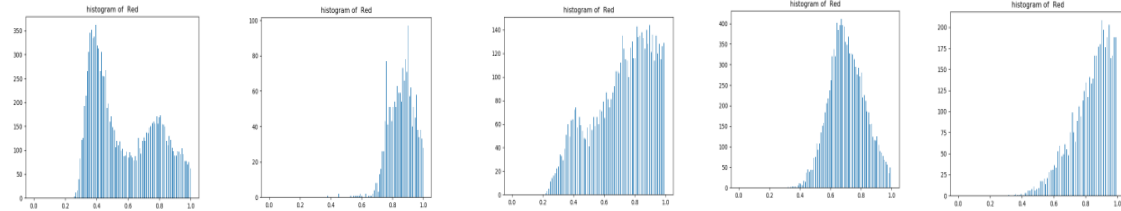
Fig. 2. Histograms of the gray, red, green, and blue color space for the fruit images of different diseases



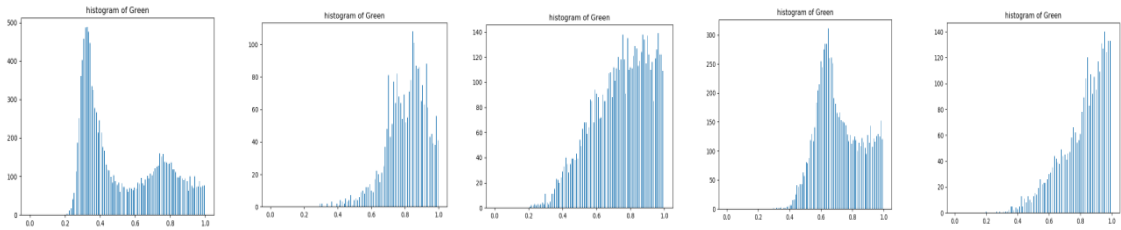
(a) Necrotic Soaked Spots Chlorosis Light green Necrosis Spot White patches spot



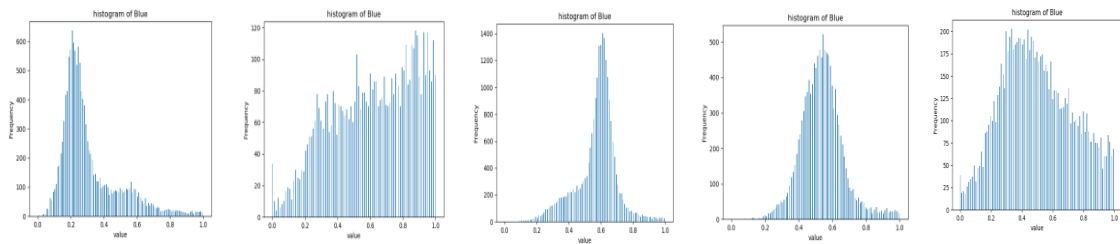
(b) Histograms of gray color space for the images in (a).



(c) Histograms of R color space for all the images in (a)



(d) Histograms of G color space for all the images in (a)



(e) Histograms of B color space for all the images in (a)

Fig. 3. Histograms of the gray, red, green, and blue color space for the leaf's images of different diseases

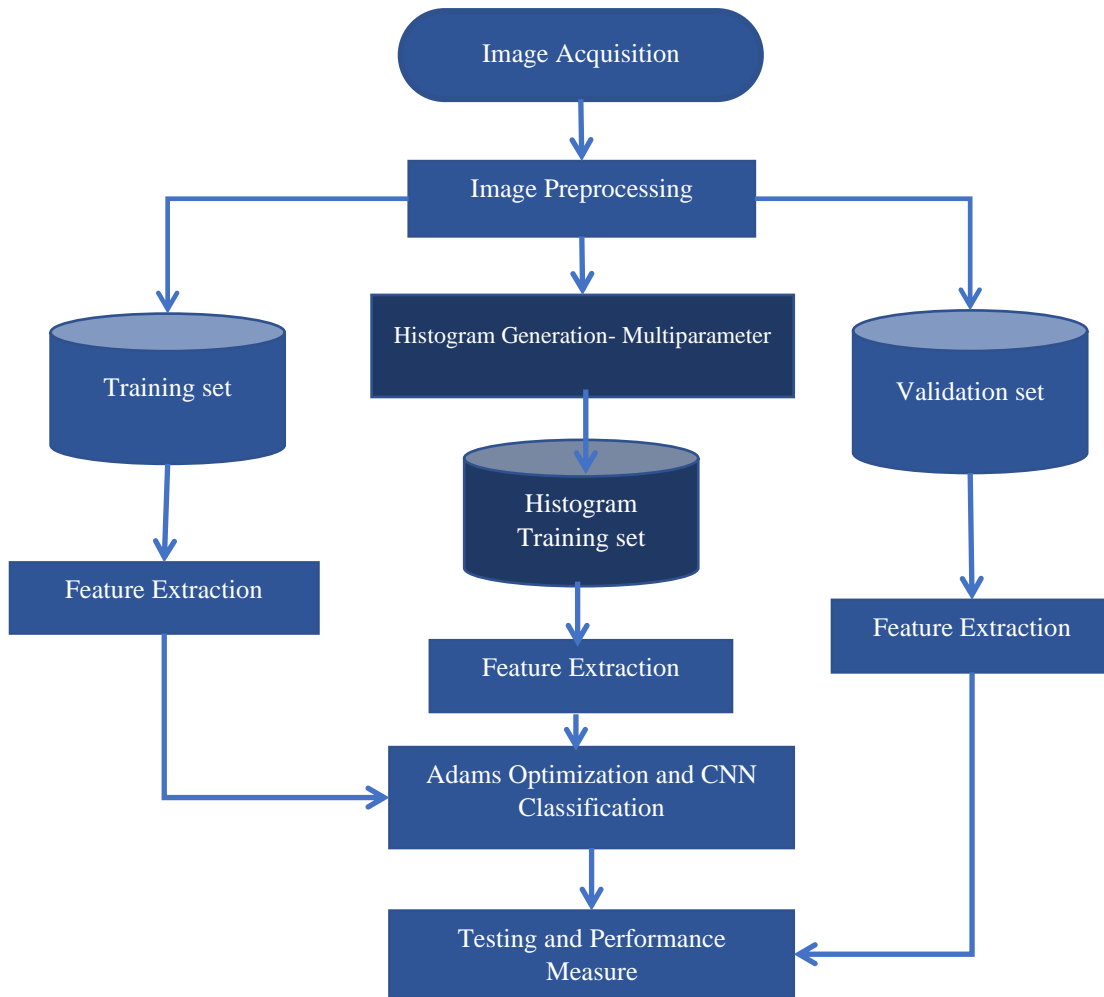


Fig. 4. Block diagram of the proposed work

3.1. Adaptive Histogram Based Features

For the input images shown in Fig. 5(a), the histograms are generated for R, G, B and gray images as shown in Fig. 5(b), where it can be seen that each histogram distribution is different for the input image. This indicates that each histogram captures some essence of the input images. The distance between the histograms of R, G, and B with the histogram of the gray image is estimated, which outputs three distance features, D-R, D-G, and D-B as defined in Equation (1)-Equation (3). Similarly, the highest peak in the histogram is selected as shown in Fig. 5(c), where we can see each highest peak represents unique behavior. The distance between the highest peaks of respective R, G, and B with the highest peak of the gray histogram is estimated, which outputs three more features, namely, Peak-R, Peak-G, and Peak-B as defined in Equation (4)-Equation (6). Since the problem is complex, the extracted six features are not sufficient for successful classification. Therefore, the proposed work divides the histograms into two equal halves, namely, P1 and P2 as shown in Fig. 5(d), where it is noted that parts of the histogram are unique for the input images of class Deep Splitting. The method repeats the same steps of estimating the

distance between P1 of respective R, G, B, and P1 of gray histograms, which results in three more features, namely, P1-R, P1-G and P1-B as defined in Equation (7)-Equation (9). In the same way, the distance between P1 of respective of R, G, and B, and the P2 of the gray histogram is estimated, which gives three more features, namely, P2-R, P2-G, and P2-B as defined in Equation (10)-Equation (12). Therefore, in total, 12 feature, which is defined as a feature vector (3+3+3+3).

For the input leaf image of class, Necrotic Soaked Spots shown in Fig. 6(a), the method draws histograms of R, G, and B, and gray images as shown in Fig. 6(b), where it can be seen each histogram distribution represent a unique pattern. In the same way, the highest peak in histograms of R, G, and B, and gray images are shown in Fig. 6(c), where the behavior of each peak is different. Dividing the histograms of R, G, B, and Gray into two equal halves as shown in Fig. 6(d), where one can notice that each part of respective color spaces and gray image behaves differently. For extracting such observations, the proposed method estimates the distance between color histograms and the gray histogram as mentioned above for fruit disease images. As a result, for each leaf image, the proposed method obtains 12 features, which is the same as feature extraction for the fruit image. The extracted features are fed to ANN for classification which will be discussed in the next sub-section.

$$D - R = X^2 = \frac{\sum_{i=1}^k \frac{x_i^2}{D_i} - \sum_{j=1}^k \frac{y_j^2}{R_j}}{\sum_{i=1}^k \frac{x_i^2}{D_i} + \sum_{j=1}^k \frac{y_j^2}{R_j}} \quad (1)$$

R indicates the histogram of red color space, D indicates the histogram of gray space, x_i is the i^{th} value of frequency density in D, y_i is the i^{th} value of frequency density of R, and k is the size of frequency density in the histogram.

$$D - G = X^2 = \frac{\sum_{i=1}^k \frac{x_i^2}{D_i} - \sum_{j=1}^k \frac{y_j^2}{G_j}}{\sum_{i=1}^k \frac{x_i^2}{D_i} + \sum_{j=1}^k \frac{y_j^2}{G_j}} \quad (2)$$

G indicates the histogram of green color space, D indicates the histogram of gray space, x_i is the i^{th} value of frequency density in D, y_i is the i^{th} value of frequency density of G, and k is the size of frequency density in the histogram.

$$D - B = X^2 = \frac{\sum_{i=1}^k \frac{x_i^2}{D_i} - \sum_{j=1}^k \frac{y_j^2}{B_j}}{\sum_{i=1}^k \frac{x_i^2}{D_i} + \sum_{j=1}^k \frac{y_j^2}{B_j}} \quad (3)$$

B indicates the histogram of blue color space, D indicates the histogram of gray space, x_i is the i^{th} value of frequency density in D, y_i is the i^{th} value of the frequency density of B, and k is the size of frequency density in the histogram.

$$Peak - R = \sum_{j=0}^n FR_j \times C_j \quad (4)$$

F indicates the Frequency Density of the Red color space, C is the width of the R histogram, R_i indicates the Feature value of the Frequency Density of the Red color Space (Histogram), $Peak - R$ is the highest value of the frequency density of $f()$, n is the size of the histogram.

$$Peak - G = \sum_{j=0}^n FG_j \times C_j \quad (5)$$

F indicates the Frequency Density of the Green color space, C is the width of the G histogram, G_i indicates the Feature value of the Frequency Density of the Green color Space (Histogram), $Peak - G$ is the highest value of the frequency density of $f()$, n is the size of the histogram.

$$Peak - B = \sum_{j=0}^n FB_j \times C_j \quad (6)$$

F indicates the Frequency Density of the blue color space, C is the width of the B histogram, B_i indicates the Feature value of the Frequency Density of the Blue color Space (Histogram), $Peak - B$ is the highest value of the frequency density of $f()$, n is the size of the histogram.

$$P1 - R = X^2 = \sum_{i=1}^{\frac{k}{2}} \frac{x_i^2}{D1_i} - \sum_{j=1}^{\frac{k}{2}} \frac{y_j^2}{R1_j} / \sum_{i=1}^{\frac{k}{2}} \frac{x_i^2}{D1_i} + \sum_{j=1}^{\frac{k}{2}} \frac{y_j^2}{R1_j} \quad (7)$$

R indicates the histogram of red color space, R1 indicates sub-part-1 of the R histogram, the D1 indicates sub-part-1 of the gray histogram. x_i is the i^{th} value of frequency density in D1, y_i is the i^{th} value of frequency density of R1, and k is the size of frequency density in the histogram.

$$P1 - G = X^2 = \sum_{i=1}^{\frac{k}{2}} \frac{x_i^2}{D1_i} - \sum_{j=1}^{\frac{k}{2}} \frac{y_j^2}{G1_j} / \sum_{i=1}^{\frac{k}{2}} \frac{x_i^2}{D1_i} + \sum_{j=1}^{\frac{k}{2}} \frac{y_j^2}{G1_j} \quad (8)$$

G indicates the histogram of green color space, G1 indicates sub-part-1 of the G histogram, and D1 indicates sub-part-1 of the gray histogram. x_i is the i^{th} value of frequency density in D1, y_i is the i^{th} value of the frequency density of G1, and k is the size of frequency density in the histogram.

$$1 - B = X^2 = \sum_{i=1}^{\frac{k}{2}} \frac{x_i^2}{D1_i} - \sum_{j=1}^{\frac{k}{2}} \frac{y_j^2}{B1_j} / \sum_{i=1}^{\frac{k}{2}} \frac{x_i^2}{D1_i} + \sum_{j=1}^{\frac{k}{2}} \frac{y_j^2}{B1_j} \quad (9)$$

B indicates the histogram of blue color space, B1 indicates sub-part-1 of the B histogram, and D1 indicates sub-part-1 of the gray histogram. x_i is the i^{th} value of frequency density in D1, y_i is the i^{th} value of frequency density of B1, and k is the size of frequency density in the histogram.

$$P2 - R = X^2 = \sum_{i=m}^k \frac{x_i^2}{D2_i} - \sum_{j=m}^k \frac{y_j^2}{R2_j} / \sum_{i=m}^k \frac{x_i^2}{D2_i} + \sum_{j=m}^k \frac{y_j^2}{R2_j} \quad (10)$$

R indicates the histogram of red color space, R2 indicates sub-part-2 of the R histogram, and D2 indicates sub-part-1 of the gray histogram. x_i is the i^{th} value of frequency density in D2, y_i is the i^{th} value of frequency density of R2, and k is the size of frequency density in the histogram.

$$P2 - G = X^2 = \sum_{i=m}^k \frac{x_i^2}{D2_i} - \sum_{j=m}^k \frac{y_j^2}{G2_j} / \sum_{i=m}^k \frac{x_i^2}{D2_i} + \sum_{j=m}^k \frac{y_j^2}{G2_j} \quad (11)$$

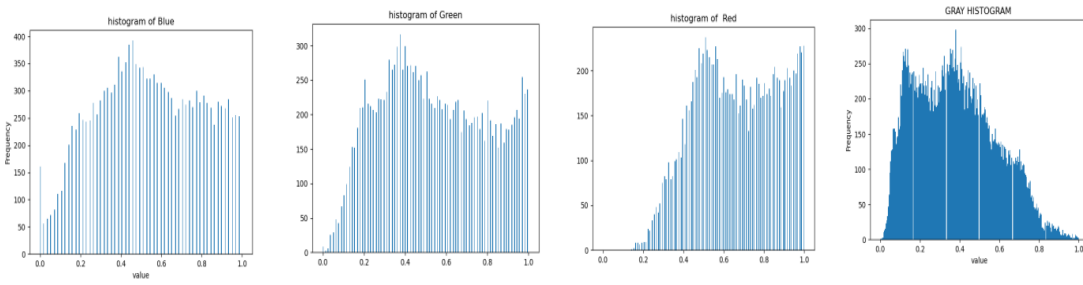
G indicates the histogram of green color space, G2 indicates sub-part-2 of the G histogram, and D2 indicates sub-part-1 of the gray histogram. x_i is the i^{th} value of frequency density in D2, y_i is the i^{th} value of the frequency density of G2, and k is the size of frequency density in the histogram.

$$P2 - B = X^2 = \sum_{i=m}^k \frac{x_i^2}{D2_i} - \sum_{j=m}^k \frac{y_j^2}{B2_j} / \sum_{i=m}^k \frac{x_i^2}{D2_i} + \sum_{j=m}^k \frac{y_j^2}{B2_j} \quad (12)$$

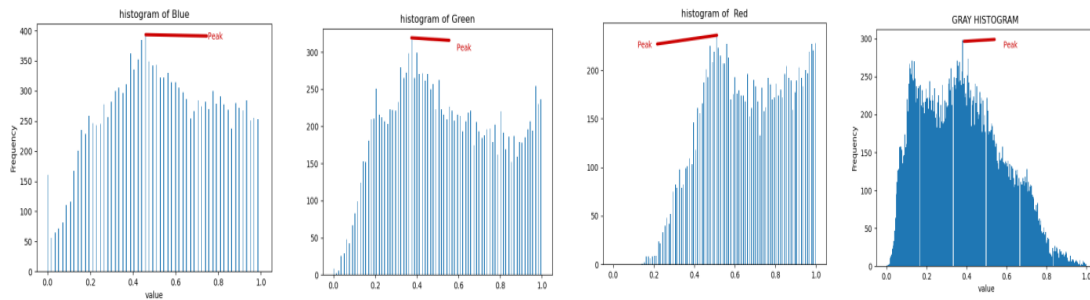
B indicates the histogram of blue color space, B2 indicates sub-part-2 of the B histogram, and D2 indicates sub-part-1 of the gray histogram. x_i is the i^{th} value of frequency density in D2, y_i is the i^{th} value of the frequency density of B2, and k is the size of frequency density in the histogram.



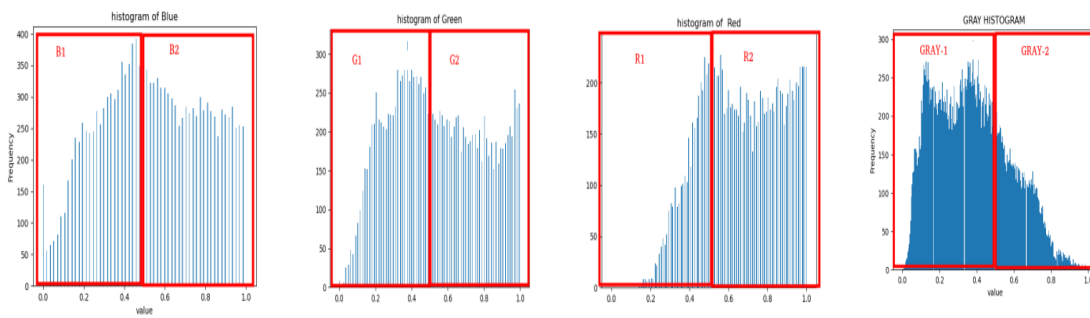
(a) Deep splitting-Class-1



(b) Histograms of R, G, B, and Gray images for a sample of the image shown in (a)



(c) Selecting the highest peak for feature extraction from the histograms in (b)

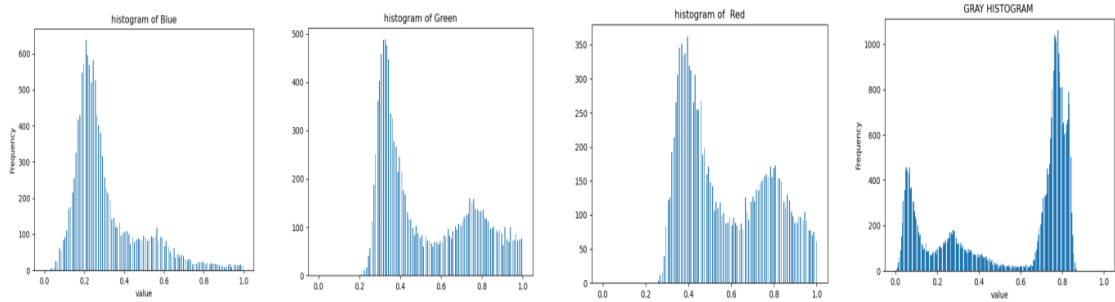


(d) Dividing the histogram into two halves (R1 and R2) for feature extraction from the histograms in (a)

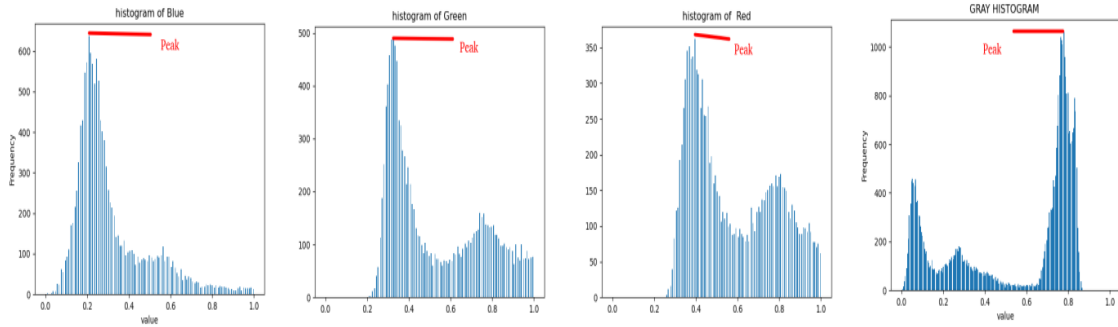
Fig. 5. Feature extraction using histogram analysis of color spaces and gray images of pomegranate fruit image shown in (a).



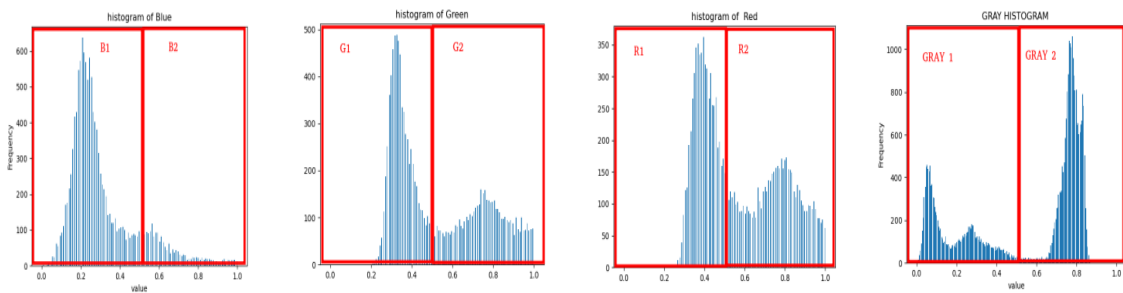
(a) Necrotic Soaked Spots -Class-1



(b) Histograms of R, G, B, and Gray images for sample leaf image shown in (a)



(c) Selecting the highest peak for feature extraction from the histograms in (b)



(d) Dividing the histogram into two halves (R1 and R2) for feature extraction

Fig. 6. Feature extraction using histogram analysis of color spaces and gray images of pomegranate leaf image shown in (a).

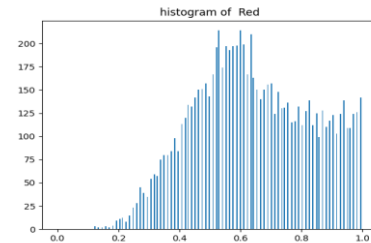
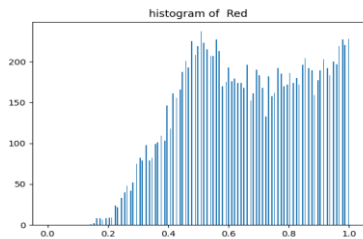
Complex Background with low quality



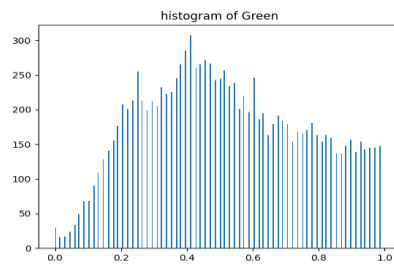
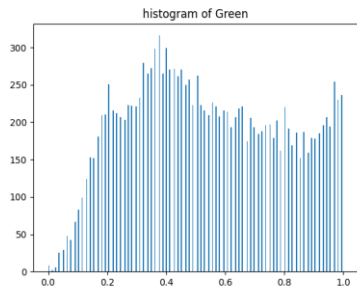
Simple background with high quality



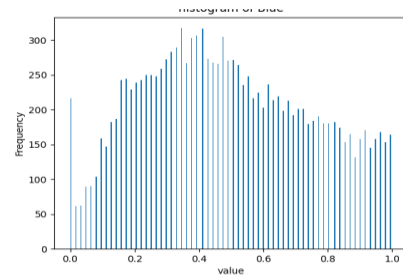
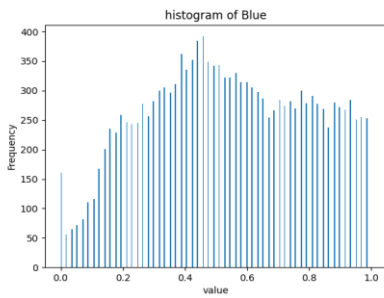
Input images



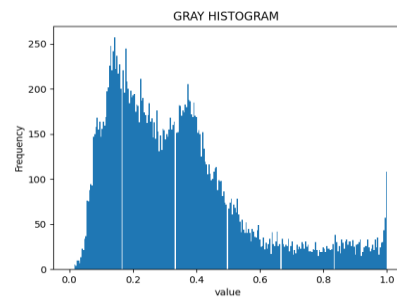
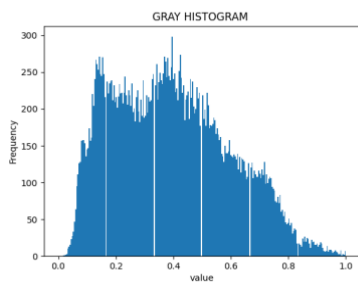
Histograms of the red color space



Histograms of the green color space



Histograms of the blue color space



Histograms of gray images of the input images

Fig. 7. Stable histogram behavior for the complex and simple background images

Complex background and Clean background

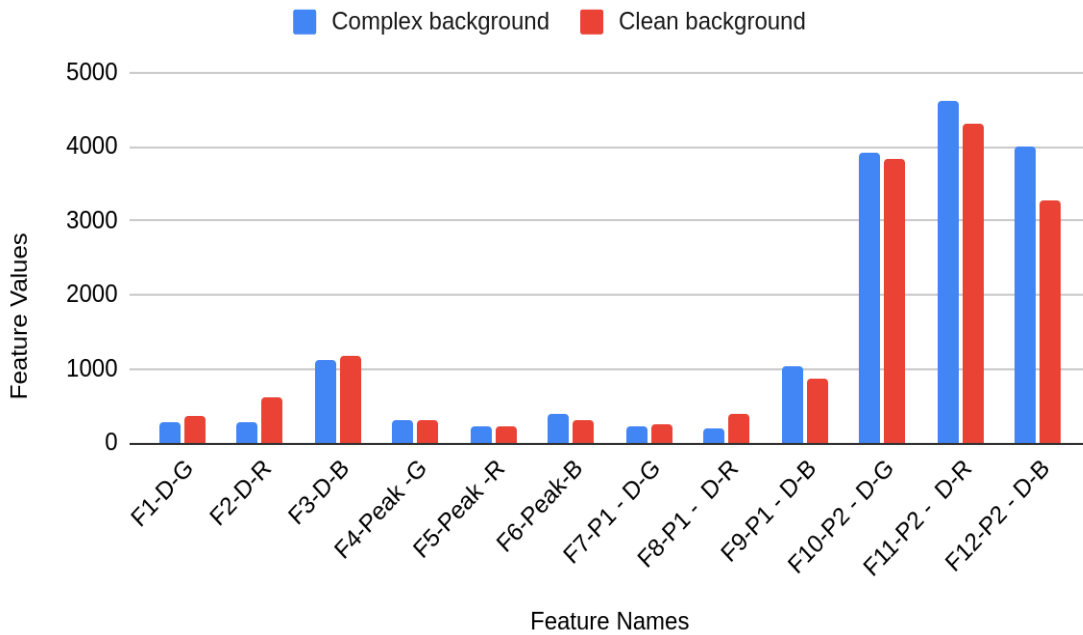
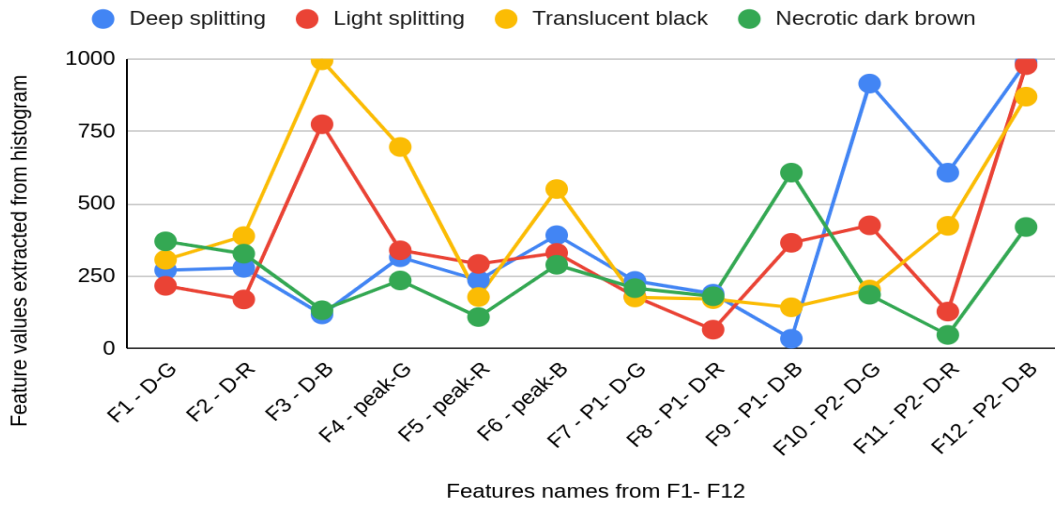


Fig. 8. Robustness of the proposed features for the images of complex and simple backgrounds

The advantage of this histogram-based approach is its robustness to image quality and background changes. It is evident from the new illustrations shown in Fig. 7 and Fig. 8, where one can see for complex and simple background input images, there is not much change in the gray histogram compared to the respective color space histograms. As result, the extracted distance-based features work well for the images of different quality and backgrounds. Therefore, the same conclusions can be drawn from Fig. 8, where the behavior of the features is similar for both complex background and simple background images.

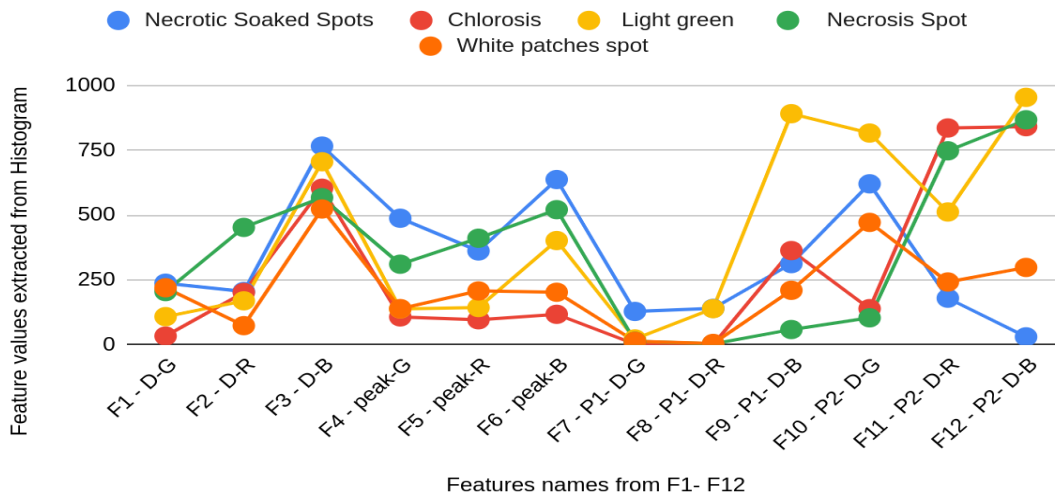
The effectiveness of the feature extraction for fruit disease classification is illustrated in Fig. (a), where it is clearly seen that the line behavior of each class is different and unique. This shows that the extracted 12 features are capable of classification of five fruit disease classes. The same conclusions can be drawn from the illustration shown in Fig. 9(b) for five classes of leaf disease classification.

Fruit class Features



(a) Distribution of features vector for fruit diseases classification

Leaf Class Features



(b) Distribution of features vector for leaf disease classification

Fig. 9. Domain independent features analysis for fruits and leaves disease classification.

3.2. Classification of Diseases of Fruits and Leaf Images

As noted in the previous section, the extracted features have sufficient discriminative power for the classification of four classes of fruit diseases and five classes of leaf diseases. Therefore, the proposed work uses Artificial Neural Networks (ANNs) for classification rather than proposing deep learning models [34-36]. The ANN uses a convolution neural network, specifically the Multilayer Perceptron (MLP), which consists of an input layer, hidden layers, and an output layer as shown in Fig. 10, where one can see details of ANN for the classification of four and five classes of fruit and leaf diseases, respectively.

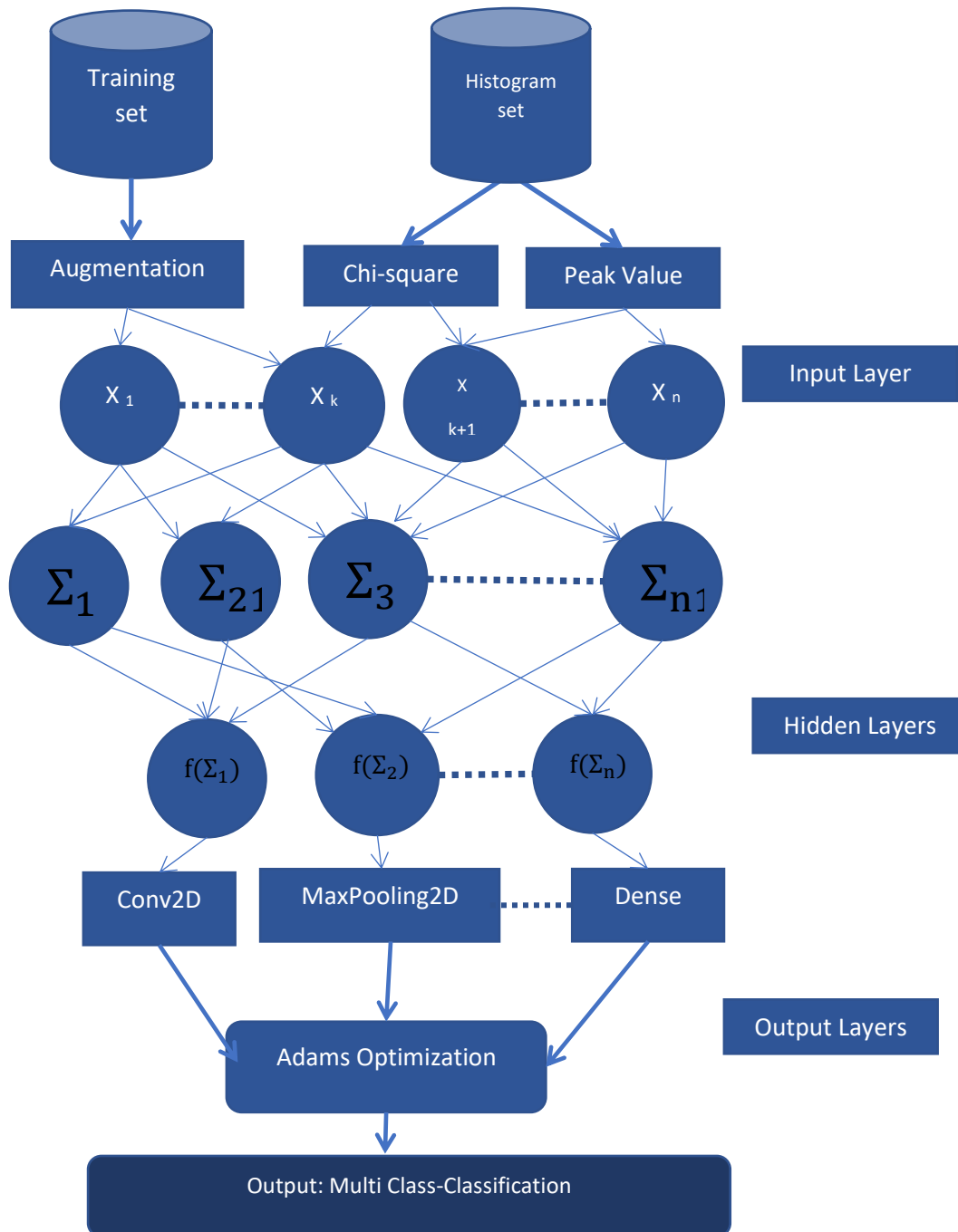


Fig. 10. ANN architecture for classification of fruit and leaves diseases

Input Layer: The input layer receives the initial input data, which are 12 features extracted from the Histogram of individual input images. Each input node represents a feature or attribute of the data. **Hidden Layers:** Between the input and output layers, here we used 2 hidden layers. Each hidden layer consists of multiple artificial neurons or units. Hidden layers help the network learn complex representations and extract higher-level features from the input data. It identifies 1,659,081(trainable) shape features by giving histogram features along with the dataset. **Output Layer:** The output layer provides the final classification of the neural network. With the available

validation set accuracy of the method is evaluated. This method is a multi-class classification, the fruits class are 4. And leaf classes are 5 method validation is done separately for these classes. The sigmoid activation function is used for classification. **Connections and Weights:** Each neuron in one layer is connected to every neuron in the subsequent layer. Each connection between neurons has an associated weight that determines the strength or importance of the connection. During the training process, the network learns optimal weights that minimize the error or loss between the predicted output and the actual output. **Activation Functions:** Activation functions introduce non-linearity into the network, enabling it to learn complex relationships between inputs and outputs.

4. Experimental Results

For evaluating the proposed method, we collected a dataset from the Biotechnology Department, where researchers are using the same images for studying infections and various causes of the diseases. They are focusing on the micro level for studying viruses and bacteria to find remedies for diseases. However, this manual process requires more time and hence it is difficult to handle a large variety of images affected by different diseases. Our work is to develop an automatic system for disease classification to assist Biotechnology experts in carrying out their own research. We verified the images we collected with help from experts in the biotechnology department. To make the dataset as comprehensive and representative as possible, the images were collected from different sources, regions and fields, open environments, and under various weather conditions. Sample images illustrating the wide diversity of inputs are shown in Fig. 11.

4.1. Dataset Creation and Evaluation

As mentioned in the previous section, the collected images of different diseases are annotated with the help of biotechnology experts. In total, for each class of fruit diseases, we collected 500 images, 2000 samples for four classes of pomegranate fruits, and 2500 samples for five classes of leaves. Sample images of four types of disease classes of fruits and five types of disease classes are shown in Fig. 11(a) and Fig. 11(b), respectively. It is noted from Fig. 11(a) and Fig. 11(b) that the patches' shape, color, and quality of the images share the same properties. At the same time, one can see from Fig. 11(a) and Fig. 11(b) that images of intra-classes have variations in color, patch shapes, and quality of the images while images of inter-classes share common properties, such as color, shape of the patches and quality of the image. This makes classification problems challenging. In the same way, our dataset includes multiple views of the same fruit/leaf

and the images affected by distortion (fruit/leaf is bad quality) as shown in Fig. 11(c). The dataset and code are available at¹

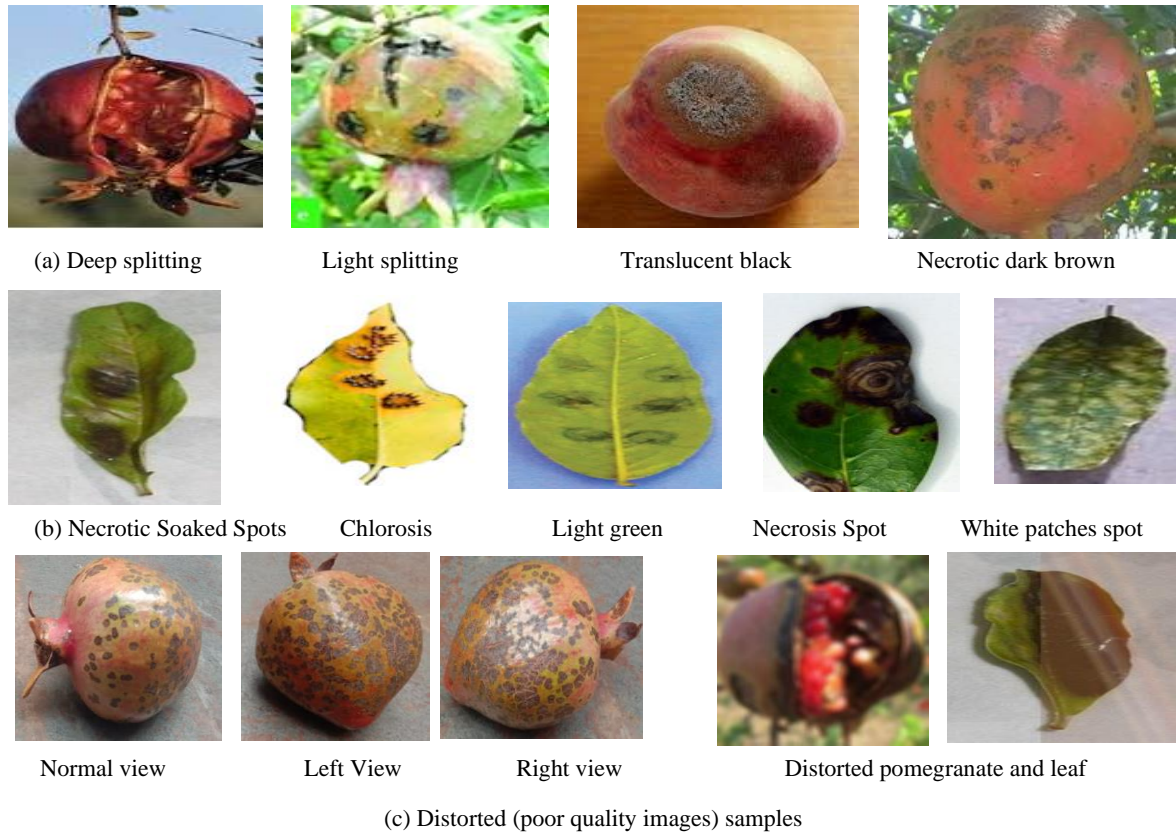


Fig 11. Sample images of different diseases from our fruit and leaf datasets. Example of successful classification of the proposed method. (a)-(b) referring to normal samples and (c) referring to distorted samples.

To show the effectiveness of the proposed model, we implement two state-of-the-art techniques, namely, Mallikarjuna et al. [20], which developed a model for arecanut disease classification using the combination of gradient feature and deep learning models. Gom-OS [26] proposed a model for the classification of different fruits based on the combination of color and depth information. The reason to choose an approach [20] for comparative study is that the objective of the method is the same as the proposed method. In addition, the technique uses a combination of feature extraction and deep learning for the classification of arecanut diseases. Furthermore, the effect of arecanut diseases is almost the same as pomegranate diseases. Therefore, the comparative study with the approach [20] is a fair comparative study with the proposed method. Similarly, the technique [26] explores color information for classifying different fruits. To show that an approach which is developed for the classification of normal fruit images may not be effective for the classification disease images, we compare the proposed method with the existing

¹<https://github.com/prajwalkumarprof/Domain-Independent-Adaptive-Histogram-Based-Approach->

approaches of fruit classification [26]. Further, for comparison purposes, we implemented several deep learning-based models [21-24], which focus on the objects in the images for feature extraction and classification.

For evaluating the performance of the proposed method, we use the confusion matrix and Average Classification Rate (ACR), which is the mean of diagonal elements of the confusion matrices. For generating a confusion matrix, we employ 10-fold cross-validation, which chooses the number of training and testing samples automatically. The average of 10 confusion matrices is considered the final confusion matrix for validating the performance of the methods.

4.2. Ablation Study

For the successful classification of different diseases of pomegranate fruits and leaves, the way the proposed work extracts features using a histogram of color space and gray images is vital. Therefore, to show the contribution of 12 features, we calculated ACR for each feature on a dataset of fruit and leaves and the results are reported in Table 1. The extracted 12 features are defined as follows. Furthermore, the SVM and KNN classifiers are classical models and well-known classifiers for classification, detection, and identification [30, 31]. Similarly, XGBoost is a well-known deep-learning model, and it has been used for classification in several fields. To show that the proposed method with ANN is the best for the classification of different disease classes of pomegranate fruits and leaves, the ACR is calculated for the proposed method with the different models mentioned above. The results are reported in Table 1.

- (i) D-R (the distance between the histogram of R space and the histogram of the gray image).
- (ii) D-G (the distance between the histogram of G space and the histogram of the gray image).
- (iii) D-B (the distance between the histogram of B space and the histogram of the gray image).
- (iv) Peak-R (the distance between the peak in the histogram of R space and the peak in the histogram of the gray image).
- (v) Peak-G (the distance between the peak in the histogram of G space and the peak in the histogram of the gray image).
- (vi) Peak-B (the distance between the peak in the histogram of B space and the peak in the histogram of the gray image).
- (vii) P1-D-R (the distance between Part-1 (P1) of the histogram of R space and the P1 of the histogram of the gray image).
- (viii) P1-D-G (the distance between Part-1 (P1) of the histogram of G space and the P1 of the histogram of the gray image).

- (ix) P1-D-B (the distance between Part-1 (P1) of the histogram of B space and the P1 of the histogram of the gray image).
- (x) P2-D-R (the distance between Part-2 (P2) of the histogram of R space and the P2 of the histogram of the gray image).
- (xi) P2-D-G (the distance between Part-2 (P2) of the histogram of G space and the P2 of the histogram of the gray image).
- (xii) P2-D-B (the distance between Part-2 (P2) of the histogram of B space and the P2 of the histogram of the gray image).
- (xiii) The Proposed method with SVM. In this experiment, the ANN has been replaced with an SVM classifier with the same set-up experiments for classification.
- (xiv) The Proposed method with KNN. Here, the ANN of the proposed method is replaced by KNN with the same experimental setup for classification.
- (xv) The Proposed method with XGBoost. In this case, the ANN is replaced by the XGBoost model for classification.

Table 1. Average Classification Rate (ACR) of the key features for fruit and leaf diseases

#	Feature	Fruit class		Leaf class	
		ACR-without Augmentation	ACR-with Augmentation	ACR-without Augmentation	ACR-with Augmentation
(i)	D-G	18.64	24.08	29.47	30.20
(ii)	D-B	54.01	13.75	18.64	20.24
(iii)	D-R	22.60	36.15	21.01	26.56
(iv)	Peak-G	21.41	20.96	41.15	42.25
(v)	Peak-B	35.78	29.75	29.62	31.08
(vi)	Peak-R	21.16	26.43	22.11	23.96
(vii)	P1 D-G	22.50	29.92	70.34	70.39
(viii)	P1 D-B	10.90	31.77	48.39	48.40
(ix)	P1 D-R	17.00	51.18	47.82	48.03
(x)	P2 D-G	58.00	47.71	21.56	36.11
(xi)	P2 D-B	36.45	73.02	21.91	42.27
(xii)	P2 D-R	51.35	68.37	5.73	19.43
(xiii)	SVM	77.10	96.49	82.00	98.00
(xiv)	K-NN	71.28	90.10	86.01	93.01
(xv)	XGBoost	77.95	88.67	76.69	95.80
(xvi)	Proposed	84.10	98.55	89.32	99.20

As mentioned earlier, collecting real data for different diseases is not easy, so to increase the number of samples, we use different augmentation techniques such as rotation, scaling, flipping, etc. When we train the ANN model with samples, the classification performance increases. To show the effectiveness of the augmentation, we report ACR for classification with augmentation and without augmentation in Table 1. It is noted from Table 1 that for most of the feature

extraction steps, the ACR with augmentation is higher than ACR without augmentation. It can be validated with the results of ACR of the proposed method with augmentation and without augmentation. The ACR of the proposed method without augmentation is higher than the proposed method without augmentation. Therefore, one can infer that augmentation improves the classification performance for both fruits and leaves images. In the same way, the results of each feature extraction step reported on both the fruit and leaves datasets in Table 1 show that each step contributes to achieving the best results of the proposed method. It is evident from the ACR of the proposed method on fruits and leaves images of different diseases.

It is noted from experimental results (xiii, xiv, xv, and xvi) that for the classification of images of different diseases of fruit and leaves, the proposed method with ANN is better than the proposed method with SVM, KNN and XGBoost models. This shows that the combination of the proposed feature + ANN is robust to different domains while the proposed method with SVM, KNN and XGBoost is not. When we analyze the results of the SVM, KNN, and XGBoost models, the performance of the XGBoost model is poor compared to the other methods on both the datasets. This makes sense because XGBoost model requires a large number of samples for achieving the best results [33]. On the other hand, SVM and KNN perform well with a smaller number of samples.

4.3. Experiments on Fruit and Leaf Disease Classification

Qualitative results of the proposed method for the classification of different diseases of pomegranate fruits are shown in Fig. 11(a), where it can be seen that the proposed method is capable of classifying images affected by different diseases accurately. The same conclusions can be drawn from the quantitative results of the proposed method on the fruit dataset reported in Table 2, where it is noted that our model achieves 84.10 ACR for the classification of different diseases of pomegranate fruits.

Table 2. Confusion matrix and ACR (in %) of the proposed method on fruit disease classification

Fruit classes	Deep splitting	Light splitting	Translucent black	Necrotic dark brown
Deep splitting	369	49	49	73
Light splitting	180	565	73	172
Translucent black	74	50	287	97
Necrotic dark brown	367	146	109	558
ACR	84.10			

Qualitative results of the proposed method for the classification of different diseases of pomegranate leaves are shown in Fig. 11(b), where it is noted that the method classifies successfully through images that share common properties. This indicates that the proposed method has the ability to classify leaves images of different diseases. Quantitative results of the

proposed and existing methods for the classification of different diseases on the leaves dataset are reported in Table 3, where it is noted that the proposed model achieves promising classification rate for all the classes. Therefore, we can conclude that the proposed method is domain independent.

Table 3. Confusion matrix and ACR (in %) of the proposed method on leaves disease classification

Leaf classes	Necrotic soaked spots	Chlorosis	Light green spots	Necrosis	White patches
Necrotic soaked spots	558	248	306	90	238
Chlorosis	184	378	76	40	76
Light green spots	54	393	144	76	32
Necrosis	10	44	22	328	140
White patches	162	86	76	162	594
ACR	89.32				

4.4. Comparative Study with State-of-the-Art

The performance of our proposed method is compared with the results of existing methods [20-24, 26] as reported in Table 4 on both disease classification datasets. As can be seen, our method outperforms the existing methods in terms of ACR. We believe the existing methods perform poorly because their features are not robust compared to the features we have designed. It is also the case that these methods were not developed specifically for pomegranate fruit and leaf disease classification. While method [20] was developed for classifying diseases in arecanuts, which bear some resemblance to pomegranates, the method is not competitive with what we have proposed. Similarly, the methods [21-24, 26] were developed for the classification of images and objects based on deep learning, the methods do not perform well compared the proposed method.

Our method achieves better ACR for the leaf dataset compared to the fruit dataset. This is in spite of leaf disease classification being a five-class problem in contrast to the four-class problem of fruit diseases. The fruit images have complex backgrounds while the leaf images do not, which may explain this. Overall, the performance of the proposed method for the classification of fruit and leaf diseases is promising and hence, the proposed method is domain independent.

To show that our method is invariant to rotation, scaling, and to some extent to blur and noise, we tested all of the methods on examples of such images. The results are reported in Table 5. We note that the average accuracy on the normal images, rotated images, and scaled images is almost the same. This shows invariance to rotation and scaling. However, for the distorted images, the average accuracy of the proposed method is somewhat lower than the average accuracy on normal images. The reason may be that the effects of distortion resemble the damage caused by diseases.

Table 4. The average accuracy of the proposed and existing methods on fruit and leaf diseased datasets (in %)

Methods	Accuracy	
	Fruit Class	Leaf Class
Proposed method	98.55	99.20
Mallikarjun et al. [20]	85.33	86.76
Gom Os et al. [26]	86.00	88.00
Petersen et al. [21]	88.37	90.66
Li et al. [22]	88.80	88.16
He et al. [23]	77.16	78.32
Chrysos et al. [24]	71.26	74.23

Table 5. The average accuracy of the proposed and existing methods on scaled, rotated, and distorted images

Methods	Scaled Up and Down		Rotated in Different Angles		Distorted (different levels of Gaussian noise and blur)	
	Fruit class	Leaf class	Fruit class	Leaf class	Fruit class	Leaf class
Proposed method	98.3	99.01	97.2	99.12	89.23	92.39
Mallikarjun et al. [20]	85.33	86.76	82.45	84.76	81.42	84.34
Gom Os et al. [26]	86.00	88.23	85.56	87.53	84.45	84.77
Petersen et al. [21]	88.37	88.37	86.12	89.54	74.52	75.66
Li et al. [22]	88.8	88.2	86.53	86.41	72.62	71.65
He et al. [23]	77.16	76.08	72.81	75.55	66.57	65.49
Chrysos et al. [24]	71.6	72.01	71.82	72.54	61.51	62.78

To show that the proposed method is computationally efficient, we calculate the response time per image in seconds for all the methods on both datasets and report these results in Table 6. We note that our approach outperforms the others in nearly all cases. Since the existing models involve expensive classifiers and models, they demand significant processing time. For our experiments, we employed the following software and hardware components: **Software:** OS : Linux Mint 21.0 Mate, Editor : VSCODE 1.85, Python : 3.10.12, **Hardware:** Processor -AMD Ryzen 3200G @3.6GHz, Ram : 8GB, HDD : 1TB.

Table 6. The response time per image in seconds of the proposed and existing methods on fruit and leaf image datasets

Methods	Response Time	
	Fruit class	Leaf class
Proposed method	0.26	0.29
Mallikarjun et al. [20]	0.36	0.44
Gom Os et al. [26]	0.25	0.42
Petersen et al. [21]	1.09	1.3
Li et al. [22]	0.82	1.2
He et al. [23]	0.53	0.62
Chrysos et al. [24]	0.27	0.37

Although our dataset includes multiple views of the same fruit/leaf, sometimes, the photographs miss disease patches. In this case, our method will not work. To overcome this problem, we could use a 3D imaging technique or combine all the 2D views of the same fruit/leaf. It is no doubt better to process multiple views to locate diseases patches and then fuse the information extracted for the final classification. This seems like an interesting topic for future research.

Similarly, sometimes, when the images are affected by other adverse factors such as noise, degradations, loss of patch shapes and color information, the proposed method does not work well, as shown in sample cases in Fig. 12. In Fig. 12, the proposed method misclassifies the image of deep splitting as a light splitting class. In the same way, the image of the white patches class is misclassified as the light green spot class. This is because the presence of leaves in the fruit image and the confusion between white and green patches leads to misclassification. Therefore, there is scope for improving our proposed method. To address this challenge, we plan to introduce the spatial relationship between the pixels (new attention mechanism) to extract high-level features, which are invariant to shape, distortion, and loss of information.



Deep splitting -Light Splitting



White Patches-Light green spots

Fig. 12. Example for misclassification of fruit and leaf dataset.

5. Conclusion and Future Work

We have proposed a new method for the classification of different diseases of pomegranate fruits and leaves. The model works based on an adaptive histogram approach. The histograms are used for extracting distance-based features by comparing the histogram of color spaces with the histogram of gray images. To strengthen the feature extraction, we detect the highest peak in the histograms for extracting distance-based features. In the same way, the histograms are divided into two equal parts at the center of the distribution. Then the sub-parts are used for extracting distance-based features. The features are supplied to Artificial Neural Network for classification. The results on fruit and leaf datasets show that the proposed method is domain independent and outperforms existing methods in terms of ACR. However, for some of the images shown in Fig. 12, the performance of the method degrades. To solve this problem, we plan to explore deep learning models with new attention mechanisms in the future. Furthermore, to address missed disease patches in different views of the same fruit/leaf, it is necessary to develop a method which can locate disease patterns across a number of views and fuse this information for making an identification.

Acknowledgments

References

1. P. Kumar, M. S. Dashya, P. Doddararju. B. S. Meti and M. Gligowda, Differential gene responses in different varieties of pomegranate during the pathogenesis of *Xanthomonas axonopodis* pv. *Punicae*. Biotech, Springer, 2021.
2. J. Sharma et al. Genetic diversity and streptomycin sensitivity in *Xanthomonas axonopodis* pv. *Punicae* causing oily spot disease in pomegranate. Horticulture, MDPI, 2022.
3. L. Vauterin, B. Haste, K. Kersters and J. Swings, Reclassification of *Xanthomonas*. Int. J. Syst. Bacterial., 45: 475-489, 1995.
4. R. Chandra, V. T. Jadhav and J. Sharma, Global Scenario of pomegranate (*Punica granatum* L.) culture with special reference to India, Fruit vegetable and cereal science and Biotechnology, pp 7-18, 2010.

5. L. Czieczor, C. Bentkamp, L. Damerow and M. Blanke, Non-invasive determination of the quality of pomegranate fruit, *Postharvest Biology and Technology*, pp 74-79, 2018.
6. M. Palumbo, M. Cefoloa, B. Pace, G. Attolico and G. Colelli, Computer vision system based on conventional imaging for non-destructively evaluating quality attributes in fresh and packaged fruit and vegetables, *Postharvest Biology and Technology*, 2023.
7. H. Azgomo, F. R. Haredashi and M. R. S. Motlagh, Diagnosis of some apple fruit disease by using image processing and artificial neural network, *Food Control*, 2023.
8. Y. Grurubelli, M. Ramanathan and P. Ponnusamy, Fractional fuzzy 2DLDA approach for pomegranate fruit grade classification, *Computer and Electronics in Agriculture*, pp 95-105, 2019.
9. C. S. Yin, N. Juan, C. Da, L. H. Xian X. Hui, C. L. Na, Z. F. Hong and Z. D. Guang, Comparative proteomics analysis of pomegranate seeds in fruit maturation period, *Journal of Integrative Agriculture*, pp 2558-2564, 2015.
10. S. Janati, S. A. Mehdizadeh and M. Heydari, Designing manufacturing and evaluating the diagnosis system of carob moth in pomegranate fruit using digital image processing, *Computers and Electronics in Agriculture*, 2022.
11. A. Umamageswari, S. Deepa an K. Raja, An enhanced approach for leaf disease identification and classification using deep learning, *Measurements: Sensors*, 2022.
12. A. Pandey and K. Jain, A robust deep attention dense convolutional neural network for plant leaf disease identification and classification from smart phone captured real world images, *Ecological Informatics*, 2022.
13. R. Karthickmanog, J. Padmapriya and T. Sasilatha, A novel pixel replacement-based segmentation and double feature extraction techniques for efficient classification of plant leaf diseases, *Materials Today: Proceedings*, pp 2048-2052, 2021.
14. G. Dhingra, V. Kumar and H. D. Joshi, Basil leaves disease classification and identification by incorporating survival of fittest approach, *Chemometrics and Intelligent Laboratory Systems*, pp 1-11, 2019.
15. A. Nigam, A. K. Tiwari and A. Pandey, Paddy leaf disease recognition and classification using PCA and BFO-DNN algorithm by image processing, *Materials Today: Proceedings*, pp 4856-4862, 2020.
16. P. B. Wakhare, S. Neduncheliyan and K. R. Thankur, Study of disease identification in pomegranate using leaf detection technique, In *Proc. ESCI*, pp 1-6, 2022.
17. M. D. Nirmal, Farmer friendly smart App for pomegranate disease identification, In *Proc. ICECAA*, pp 884-890, 2022.
18. M. D. Nirmal, Pomegranate leaf disease classification using feature extraction and machine learning, In *Proc. ICOSEC*, pp 619-626, 2022.
19. S. B. Mallikarjuna, P. Shivakumara, V. Khare, N. V. Kumar, M. Basavanna, U. Pal and B. Poornima, CNN based method for multi-type diseased arecanut image classification, *Malaysian Journal of Computer Science*, Vol. 34 (3), pp 255-265, 2021.
20. S. B. Mallikarjuna, P. Shivakumara, V. Khare, M. Basavanna, U. Pal and B. Poornima, Multi-gradient-direction based deep learning model for arecanut disease identification, *CAAI Transactions on Intelligence Technology*, pp 156-166, 2022.
21. F. Petersen, H. Kuehne, C. Borgelt and O. Deussen, Differentiable Top-k Classification Learning, In *Proc. PMLR*, 162, 2022.
22. Y. Li, C. Y. Wu and H. Fan, MViTv2: Improved Multiscale Vision Transformers for Classification and Detection, In *Proc. CVRP*, pp 4804-4814, 2022.
23. T. He, Z. Zhang, H. Zhang, Z. Zhang, J. Xie and M. Li, Bag of Tricks for Image Classification with Convolutional Neural Networks, In *Proc. CVPR*, pp 558-567, 2018.

24. G. G. Chrysos, M. Georgopoulos, J. Deng, J. Kossaifi, Y. Panagakis, A. Anandkumar, Augmenting Deep Classifiers with Polynomial Neural Networks, In Proc. ECCV, pp 692-716, 2022.
25. N. Pradeep, K. G. P. Raj, N. M. P. Chanduru, N. Kalaivani and N. Nandala, Fruit disease classification using convolutional neural network, In Proc. ICESC, pp 1052-1057, 2022.
26. D. F. K. Gom-Os, Fruit Classification using Colorized Depth Images, International Journal of Advanced Computer Science and Applications, Vol. 14, No. 5, pp 1023-1032, 2023.
27. P. Sajitha and A. D. Andrushia, Banana fruit disease detection and categorization using graph convolutional neural network, In Proc. ICDCS, pp 130-134, 2022.
28. M. A. Matboli and A. Atia, Fruit disease's identification and classification using deep learning model, In Proc. MIUCC, pp 432-437, 2022.
29. S. Mehta, V. Kukreja, A. Bansal, K. Kaur and A. Singh, Exploring the potential of convolutional neural network in automatic diagnosis of dragon fruit disease from plant photographs, In Proc. ICICCS, pp 536-540, 2023.
30. A. S. Nagesh and G. N. Balaji, Deep learning approach for recognition and classification of tomato fruit disease, In Proc. ICDSA AI, 2022.
31. A. Koufatzis, E. Vrochidou and G. A. Papakostas, Visual quality inspection of pomegranate crop using a novel dataset and deep learning, In Proc. IWSSIP, pp 1-4, 2022.
32. R. S. Kale and S. Shitole, Deep learning optimizer performance analysis for pomegranate fruit quality gradation, In Proc. IBSSC, 2022.
33. M. D. Nirmal, P. Jadhav, S. Pawar, M. Kharde and Pravara, Deep learning-based disease detection using pomegranate leaf image, In Proc. STCR, 2022.
34. A. Mondal, B. Mondal, A. Chakraborty, A. Kar. A. Biswas and A. B. Majumder, Heart disease prediction using support vector machine and artificial neural network, Artificial Intelligence and Applications, pp 01-07, 2023.
35. M. Hasanvand, M. Nooshyar, E. Moharamkhan and A. Selyari, Machine Learning methodology for identifying vehicles using image processing, Artificial Intelligence and Applications, pp 01-09, 2023.
36. S. Pal, A. Roy, P. Shivakumara and U. Pal, Adapting a Swin transform for license plate number and text detection in drone images, Artificial Intelligence and Applications, pp 01-10, 2023.